ACS APPLIED MATERIALS & INTERFACES

Research Article

www.acsami.org

Effect of Surface Chemical Functionalities on Collagen Deposition by Primary Human Dermal Fibroblasts

Akash Bachhuka,[†] John Hayball,[‡] Louise E. Smith,[*,†,§] and K. Vasilev[*,†,§]

[†]Mawson Institute and [§]School of EngineeringUniversity of South Australia, Adelaide, South Australia 5095, Australia

[‡]Experimental Therapeutics Laboratory, Sansom Institute and Hanson Institute, School of Pharmacy and Medical Science, University of South Australia, Adelaide, South Australia 5000, Australia

Supporting Information

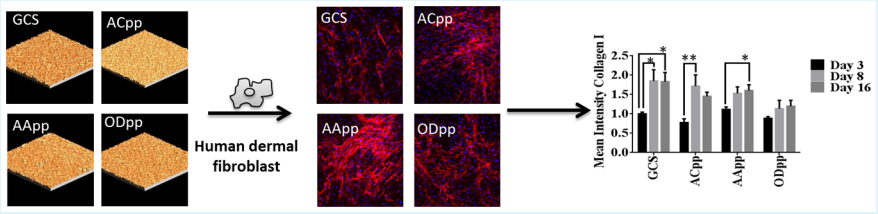

ABSTRACT: Surface modification has been identified as an important technique that could improve the response of the body to implanted medical devices. Collagen production by fibroblasts is known to play a vital role in wound healing and device fibrous encapsulation. However, how surface chemistry affects collagen I and III deposition by these cells has not been systematically studied. Here, we report how surface chemistry influences the deposition of collagen I and III by primary human dermal fibroblasts. Amine (NH_3), carboxyl acid (COOH), and hydrocarbon (CH_3) surfaces were generated by plasma deposition. This is a practically relevant tool to deposit a functional coating on any type of substrate material. We show that fibroblasts adhere better and proliferate faster on amine-rich surfaces. In addition, the initial collagen I and III production is greater on this type of coating. These data indicates that surface modification can be a promising route for modulating the rate and level of fibrous encapsulation and may be useful in informing the design of implantable biomedical devices to produce more predictable clinical outcomes.

KEYWORDS: *plasma polymerization, surface chemistry, collagen I, collagen III, fibroblasts*

INTRODUCTION

Advances in medical treatment and an aging population in the developed world have greatly increased the need for medical devices to improve the quality of life. Examples of such devices include joint replacements, pacemakers, biosensors, hernia meshes, artificial organs, and reconstructive implants. In the process of implanting a medical device, several biological phenomena occur including injury, hemostasis, inflammation, granulation, tissue remodeling, and sometimes the formation of a fibrous capsule, which can affect the ultimate functionality of the implant.[1−3] The fibrous capsule comprises of fibroblasts and leukocytes along with different families of collagens secreted by the fibroblasts.[3−5] In the early phase after implantation, collagen III fibers are secreted, which are thinner in diameter than collagen I and are regarded as immature collagen. Later, collagen III is replaced by more organized collagen I, which provides greater tensile strength to the healing structure.[6−9]

There are many examples of situations where the presence of a fibrous capsule can compromise implant functionality. An example is the pacemaker. Isolation of a pacemaker from the surroundings leads to an increase in impedance, which causes higher power consumption. As a result of this, batteries need to be replaced much more regularly than expected.[10] Another example is the delay in the signal from glucose sensors because of the formation of a fibrous capsule around the device.[11−14] In the case of a breast implant, growth of a fibrous capsule can cause capsule contracture which in turn leads to deformity and pain, in addition to device failure.[15] Collagen I and III also play an important role in healing the wound generated when a polymer mesh is implanted at a hernia site. In the case of an incisional hernia, the collagen I to III ratio decreases, which results in impaired wound healing. Increased production of collagen III fibers compared to collagen I fibers leads to an imbalance in the cross-linking and geometrical confirmation of collagens. This further reduces the mechanical stability of the connective tissue.[16,17] It is clear from these examples that collagen I and III play an important role in deciding the fate of implants via fibrous capsule formation.

The examples above clearly demonstrate that having the capacity to control capsule properties is a key element of successful device function and outcomes. Surface modification has been identified as an important mechanism for modulating fibrous capsule formation. However, most research efforts so far

Received: September 3, 2015
Accepted: October 12, 2015
Published: October 12, 2015

DOI: 10.1021/acsami.5b08249
ACS Appl. Mater. Interfaces 2015, 7, 23767−23775

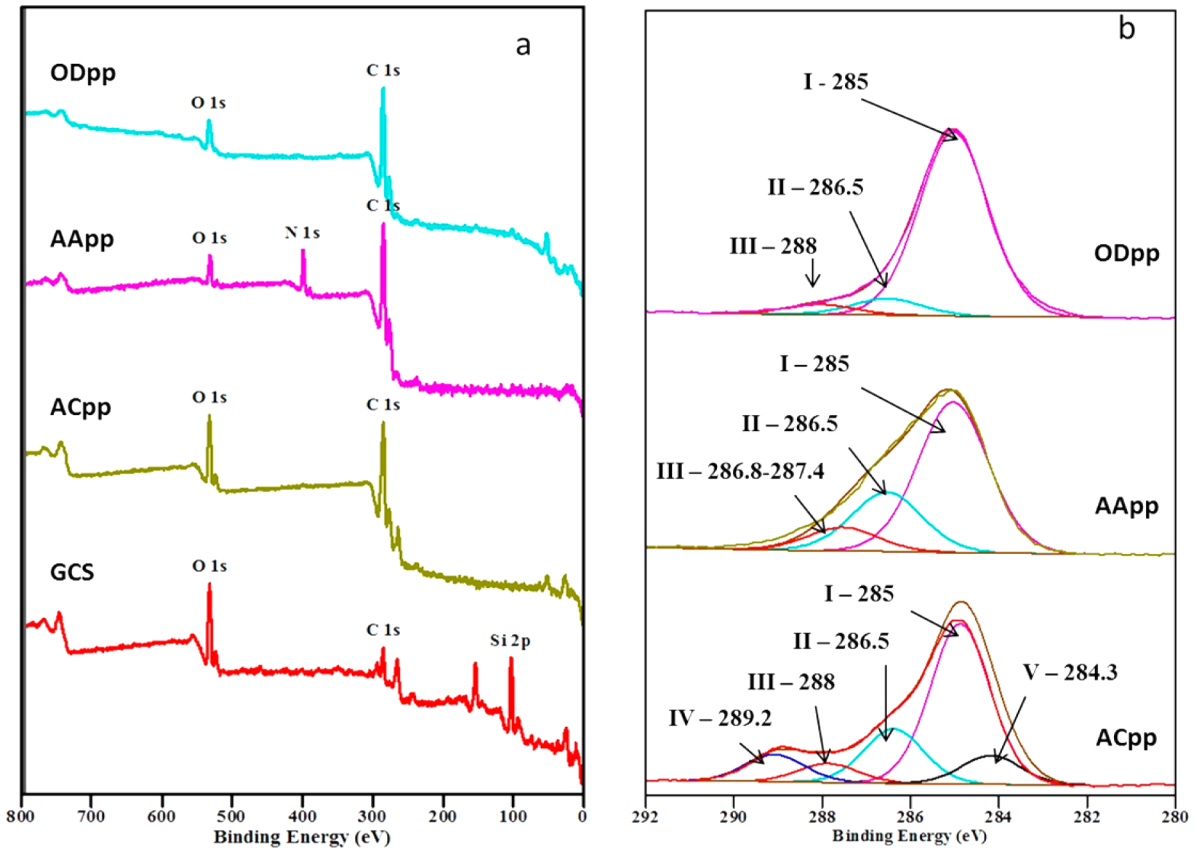

Figure 1. XPS analysis showing (a) survey spectra for unmodified glass coverslip (GCS) and plasma modified surfaces acrylic acid (ACpp), allylamine (AApp), and octadiene (ODpp). (b) C 1s spectra of chemically modified surfaces.

have been focused upon manipulating fibrous capsule formation by modulating the behavior of macrophages and leukocytes as well as the expression of pro-inflammatory cytokines by these cells.[18−20]

In this paper, we explore how surface chemistry affects the deposition of collagen I and III by primary human fibroblasts. We hypothesize that surface chemistry can be a tool to change the quantity and type of collagen deposited. This in turn could modulate the properties of the resulting fibrous capsule. We have selected coatings rich in amine (NH_3), carboxyl acid (COOH), and hydrocarbon (CH_3) functional groups, as these chemistries are the most abundant in biological tissue. The coatings have been prepared by plasma polymerization. The key benefit of plasma polymerization over other surface modification techniques is that a diverse range of pinhole-free, conformal coatings can be applied to any type of substrate material in a single-step process without the need of surface pretreatment.[21−26] In contrast, self-assembled monolayers (SAM) require specific initial chemistries, layer-by-layer (LBL) structures require charged surfaces with multiple layers and finally atomic layer deposition (ALD) can produce limited surface chemistry.[22] We have investigated the effect of these chemistries on the deposition of collagen I and III by human dermal fibroblasts over a period of 16 days. We also studied the capacity of the surface chemistries employed to modulate fibroblast adhesion and affect collagen I and III production on a cellular level.

MATERIALS AND METHODS

Materials. Allylamine (AA) (98%, Aldrich), acrylic acid (AC) (99%, Aldrich), and octadiene (OD) (98%, Aldrich) were used as received.

Plasma Polymerization. Plasma polymerization was carried out in a custom built reactor with a 13.56 MHz plasma generator.[27] Deposition of allylamine, acrylic acid, and octadiene was carried out at a pressure of 0.2 mbar and a deposition time of 2 min was employed. Power used for deposition of all three monomers was 40, 10, and 20 W, respectively. Using these conditions, we obtained polymer film of thickness of 23, 20, and 25 nm for films deposited from allylamine, acrylic acid, and octadiene, respectively. Before deposition, all substrates were cleaned by applying an air plasma for 2 min at 50 W.

X-ray Photoelectron Spectroscopy. XPS was used to determine the surface composition of the plasma polymers. All spectra were recorded using a Spec SAGE XPS spectrometer equipped with a monochromatic Mg radiation source operated at 10 kV and 20 mA. Atomic compositions of the samples were identified from survey spectra recorded over a 0−1000 eV range with pass energy of 100 eV at a resolution of 0.5 eV. All binding energies (BE) were corrected relative to a neutral C 1s carbon peak at 285.0 eV. Processing and curve fitting was performed using Casa XPS.

Atomic Force Microscopy. An NT-MDT NTEGRA SPM atomic force microscope (AFM) was used in noncontact mode to provide nanotopographical images. Silicon nitride noncontact tips coated with Au on the reflective side (NT-MDT, NSG03) were used and had resonance frequencies between 65 and 100 kHz and had spring constant between 0.35 and 6.06 N/m. The amplitude of oscillation was 10 nm, and the scan rate for 2 μm × 2 μm images was 0.5 Hz.

Water Contact Angle Measurement. Water contact angle was measured using a sessile drop method on a contact angle goniometer. Three water droplets were placed on 2 replicas of the same sample and the images were captured immediately using an adjacent camera. The

DOI: 10.1021/acsami.5b08249
ACS Appl. Mater. Interfaces 2015, 7, 23767−23775

contact angle was analyzed using ImageJ software by using Drop Snake plug-in.[28]

Cell Culture. Human dermal fibroblasts (HDFs) were harvested and grown as described previously[29] from split thickness skin samples obtained from specimens following routine breast reductions and abdominoplasties. All patients gave informed consent for skin to be used for research through a protocol approved by the Ethical Committee at the Queen Elisabeth Hospital and the University of South Australia Human Ethics Committee. Fibroblasts were grown in fibroblast culture medium (FCM) consisting of DMEM high glucose (Gibco, Life Technologies, Australia), 10% v/v fetal calf serum (FCS, Ausgenex, Australia), 100 IU/mL penicillin, and 100 μg/mL streptomycin (Gibco, Life Technologies, Australia) in an incubator at 37 °C, 5% CO_2 in a humidified atmosphere. The medium was changed every 3−4 days until the cells were 80% confluent.

Cell Seeding. Glass coverslips coated with different chemistries were then kept in 24 well plates. 50×10^3 cells were carefully seeded in 500 μL FCM and left for 1 day. The media was changed and replaced with media containing ascorbic acid (1 mM), ficoll 70 (37.5 mg/mL) and ficoll 400 (25 mg/mL) added to the media as it enhances collagen production by fibroblasts.[30−32] The media was filter sterilized and changed every 3 days until day 16.

Collagen Staining. Collagen I and III were stained on day 3, 8, and 16. Samples were washed thrice with PBS and then were fixed in ice cold methanol and left to dry. The dried plates were then washed thrice with PBS. The samples were blocked using 1% bovine serum albumin (BSA, Sigma-Aldrich) in PBS-polyethylene glycol sorbitan monolaurate (Tween 20 solution) (0.01% Tween-20 in PBS, Sigma-Aldrich) for 1 h. Next, the plates were washed thrice with PBS and a solution of primary antibody (mouse monoclonal anticollagen I and III antibody (Sigma-Aldrich) (1:1000) in blocking media was added for 90 min at room temperature. The plates were washed thrice with PBS and were incubated at room temperature using secondary antibody (Alexa flour 647 F (ab′) 2 fragment of goat anti−mouse IgG (H+L)) (Molecular probes, Life Technologies, Australia) (1:400) and counterstained with 4′, 6-diamidino-2-phenylindole (DAPI, Molecular probes, Life Technologies, Australia, λex 350 nm, λem 470 nm) (staining cell nuclei) (1:400) for 1 h in blocking media. The plates were washed thrice with PBS and then the coverslips were carefully mounted on glass slides using glycerol.

Confocal Microscopy. Confocal microscopy was used for qualitative and quantitative analysis of collagen I and III. Glass coverslips mounted on glass slides were carefully kept on the sample holder. A laser of 405 nm wavelength was employed for determining the nuclei while 640 nm wavelength laser was employed for determining collagen I and III. All samples were scanned with a 10× objective and all the parameters (laser power, pinhole size and gain) were kept constant for all the captured images. These images were analyzed using NIS-Element AR software for calculating the number of cells and area occupied by collagen per cell.

Statistical Analysis. All statistics were performed using graph pad prism 6 software. All data were expressed as mean ± standard error mean (SEM). Statistical significance was determined using a 1-way and a 2-way ANOVA with Tukey's multi comparison test. All experiments were performed twice in triplicates.

RESULTS

The surface chemical composition of the coatings deposited by plasma polymerization was thoroughly characterized by XPS. The survey spectra in Figure 1a shows that the unmodified glass surface has a silicon peak (Si 2p) along with carbon (C 1s) and oxygen (O 1s) peaks. After deposition of a plasma polymer coating the silicon peak disappeared which indicate continuous pinhole free coatings. In the case of plasma-polymerized acrylic acid (ACpp) and plasma-polymerized octadiene (ODpp), only C 1s and O 1s peaks were observed. This is consistent with the chemical composition of the precursors and published studies.[33] In the XPS survey spectra of allylamine (AApp)-coated surface, an additional peak of nitrogen (N 1s) appeared that is due to the presence of an amine group in the precursor. The deconvolution of the C 1s peaks for all the coatings are shown in Figure 1b. The C 1s spectrum of ODpp has three components: (C−H or C−C at 285.0 eV) an aliphatic carbon, (C−O at 286.5) carbon bonded to single oxygen due to O_2 contamination, and (C═O at 288) carbon double bonded to oxygen. The C 1s spectrum of AApp could also accommodate three components: one corresponding to the aliphatic carbon (C−H or C−C at 285.0 eV), the other corresponded to carbon bonded to a single nitrogen (C−NH_2, C−NH−C, and C−N═C at 286.5 eV), this peak can also include traces of C−O bonds due to oxidation. The third components can be assigned to imine (C═N) or nitrile (C≡N) groups between 286.8 and 287.4 eV. This peak can also include C═O due to O_2 contamination. C 1s spectra of ACpp can accommodate five components. The first component is assigned to aliphatic carbon (−CH) at 285.0 eV. The second one at 286.5 indicates carbon bonded to single oxygen (C-OR), the third peak at 288 indicates carbon double bonded to oxygen (−C═O), the fourth peak at 289.2 indicates a carbon bonded to two oxygen atoms such as in acid/ester groups (COOR) and the fifth at 284.3 belongs to the beta shift because of the carboxyl functionality.

Table 1 shows the atomic concentration of different elements present in the unmodified glass and glass modified with ACpp, AApp, and ODpp. 41% silicon was observed on the unmodified glass surface while no silicon was observed after modification with ACpp, AApp and ODpp. This shows that the unmodified glass surface was completely covered with the desired coating. After modification, the C/O ratio was highest for the AApp surface at 9.5, whereas the C/O ratio was lowest for ACpp surface at 3.3. The AApp coating provides a nitrogen rich chemistry, which leads to the detection of the nitrogen peak with an atomic concentration of 16.2%.

Table 1. Atomic Concentration of Chemical Elements on Bare Glass and Plasma Polymer Modified Surfaces[a]

	C 1s (at %)	N 1s (at %)	O 1s (at %)	Si 2p (at %)	C/O	N/C
GCS	19		40	41	0.47	
ACpp	76.6		23.4		3.27	
AApp	75.8	16.2	8		9.47	0.21
ODpp	88.1		11.9		7.4	

[a]All XPs data contains a standard error of 5%.

The static water contact angle of bare glass and plasma polymer modified surfaces is shown in Figure 2a. The uncoated glass coverslip was most hydrophilic with a contact angle of 15°. The plasma polymer coatings resulted in contact angles ranging from 40° to 80°, with increasing hydrophobicity ACpp < AApp < ODpp. These wettability results are consistent with previously published data where the same types of plasma polymer coatings are reported.[34] Hence, the surfaces being investigated provide not only different chemical composition but also different wetting characteristics that are known to affect biological responses. Furthermore, the modification provides differently charged coatings, as the AApp is positively charged in aqueous liquids while the ACpp is negatively charged.[34,35]

AFM imaging was carried out to analyze surface topography and morphology. Representative images of the surface of the unmodified glass and the three plasma polymer coatings are

DOI: 10.1021/acsami.5b08249
ACS Appl. Mater. Interfaces 2015, 7, 23767−23775

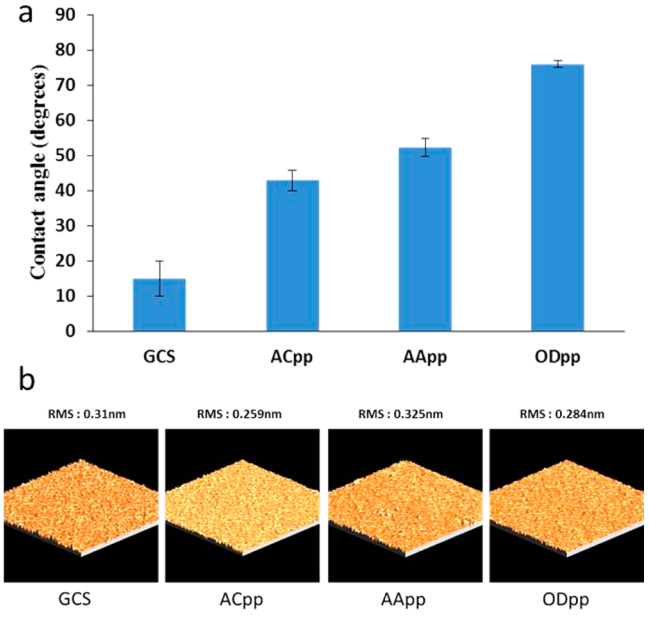

Figure 2. (a) Static water contact angles of unmodified glass coverslip (GCS) and plasma polymerized acrylic acid (ACpp), allylamine (AApp), and octadiene (ODpp). (B) AFM images and corresponding root-mean-square roughness (RMS) for different modified substrates. *X* and *Y* scale is 2 μm × 2 μm, whereas *Z* scale is 3 nm for all images.

shown in Figure 2b. Overall, all surfaces are very smooth with root-mean-square (RMS) values below 0.33 nm with no characterstic morphological features. This suggests conformal and uniform coatings.

These data demostrates that surfaces were produced with well-defined chemistry, wettability, and topography. These surfaces were further used to test for their capacity to modulate fibroblast adhesion and collagen I and III deposition.

Figure 3a shows collagen I deposition on chemically modified surfaces. The red collagen I fibers with blue primary fibroblast cell nuclei are indicated. The effect of chemistry on collagen I deposition can be visualized. On day 3, the AApp surfaces show the maximum amount of deposited collagen I compared to the other chemistries, including the uncoated glass coverslip. However, by day 8 and 16, no differences were observed between the different surfaces. This shows that chemical modification can affect the initial collagen I deposition (day 3). However, collagen I deposition saturates on all surfaces at later time points and therefore no differences are observed. Cumulatively, over 16 days, collagen I deposition increases on all the surfaces. This is expected, as more collagen I is deposited over time during the normal wound healing processes replacing the collagen III.

To support this qualitative data, we performed quantitative analysis of collagen I by analyzing the confocal microscope images using NIS-element software. Figure 3b shows a significant increase in the mean intensity of collagen I on AApp modified surfaces compared to the ACpp modified surfaces on day 3 ($p < 0.01$). However, by days 8 and 16, there was no statistically significant difference observed in the amount of collagen I deposited on both modified and unmodified surfaces (Figure 3c, d). This is in agreement with the images presented in Figure 3a. In Figure 3h, the data were further analyzed by comparing collagen I deposition over the entire 16 days. A significant increase in collagen I deposition was observed from day 3 to day 8 on the unmodified GCS ($p < 0.05$) and ACpp ($p < 0.01$). However, no significant difference was observed in AApp and ODpp surfaces. This shows that total collagen I deposition is greater on the hydrophilic (GCS and ACpp) than on the more hydrophobic (AApp and ODpp) surfaces. Additionally, a significant increase was observed in collagen I deposition from day 3 to day 16 on the unmodified GCS ($p < 0.05$) and AApp ($p < 0.05$) modified surfaces. However, no significant difference was observed in case of the ODpp surfaces. This indicates that hydrophobic surfaces can reduce collagen I deposition over a period of 16 days compared to less hydrophobic or hydrophilic surfaces.

To better understand collagen production at cellular level, we calculated the number of fibroblasts on the chemically modified surfaces and the unmodified glass coverslip (Figure S1). The AApp showed an increased number of fibroblasts compared to the other chemistries on day 3 (Figure S1a). However, there is a significant increase in the number of cells between days 3, 8, and 16 on all surfaces. All surfaces used appear to be biocompatible, with cells proliferating and achieving confluence by day 16. At early time points, the AApp appears to be the surface chemistry that promotes fibroblast growth. This is consistent with published studies.[36,37]

Collagen I deposition per cell was calculated as shown in Figure 3e–g. Although Figure 3i shows that the deposition of collagen I per cell increased steadily over the course of the 16 days of the experiment this increase was not statistically significant. Therefore, an increase in collagen I deposition could be merely due to an increase in the total cell number on these surfaces, suggesting that the factor primarily responsible for controlling the total deposition of collagen I on different chemistries is the overall number of cells.

Figure 4a shows collagen III deposition on different chemically modified surfaces. AApp surfaces produce the most collagen III compared to the other chemistries including the uncoated glass coverslip. Initially, up to day 8, collagen III production increases on all the surfaces. It then decreases between days 8 and 16. Furthermore, although collagen I appears to be deposited in the form of extracellular fibers, the collagen III appears to remain intracellular.

To support this qualitative data, we performed quantitative analysis of collagen III deposition by analyzing the confocal microscope images. Figure 4b shows that on day 3 there was a significant increase ($p < 0.0001$) in the mean intensity of collagen III on AApp surfaces compared to the unmodified GCS, and the ACpp and ODpp coated coverslips. After 8 days the AApp surface still has significantly more collagen III than the ACpp ($p < 0.05$), but not the GCS or ODpp (Figure 4c). After 16 days, there was no significant difference observed in collagen III on any of the surfaces as shown in Figure 4d. The amount of collagen III deposited per cell followed the same trend as the collagen III production, shown in Figure 4e, f, g.

In Figure 4h, the data were further analyzed by comparing the collagen III production over the entire 16 days. On the unmodified GCS the amount of collagen III increased until day 8 ($p < 0.0001$). It then decreased between days 8 and 16 ($p < 0.01$). Although the amount of collagen III increased on the ACpp and AApp over 16 days this was not statistically significant. The amount of collagen III deposited onto ODpp surfaces followed the same trend as the GCS, with an initial increase followed by a decrease between days 8 and 16; however, again this was not statistically significant.

To understand the phenomenon at a cellular level, we again collagen III production per cell calculated and plotted in Figure

DOI: 10.1021/acsami.5b08249
ACS Appl. Mater. Interfaces 2015, 7, 23767−23775

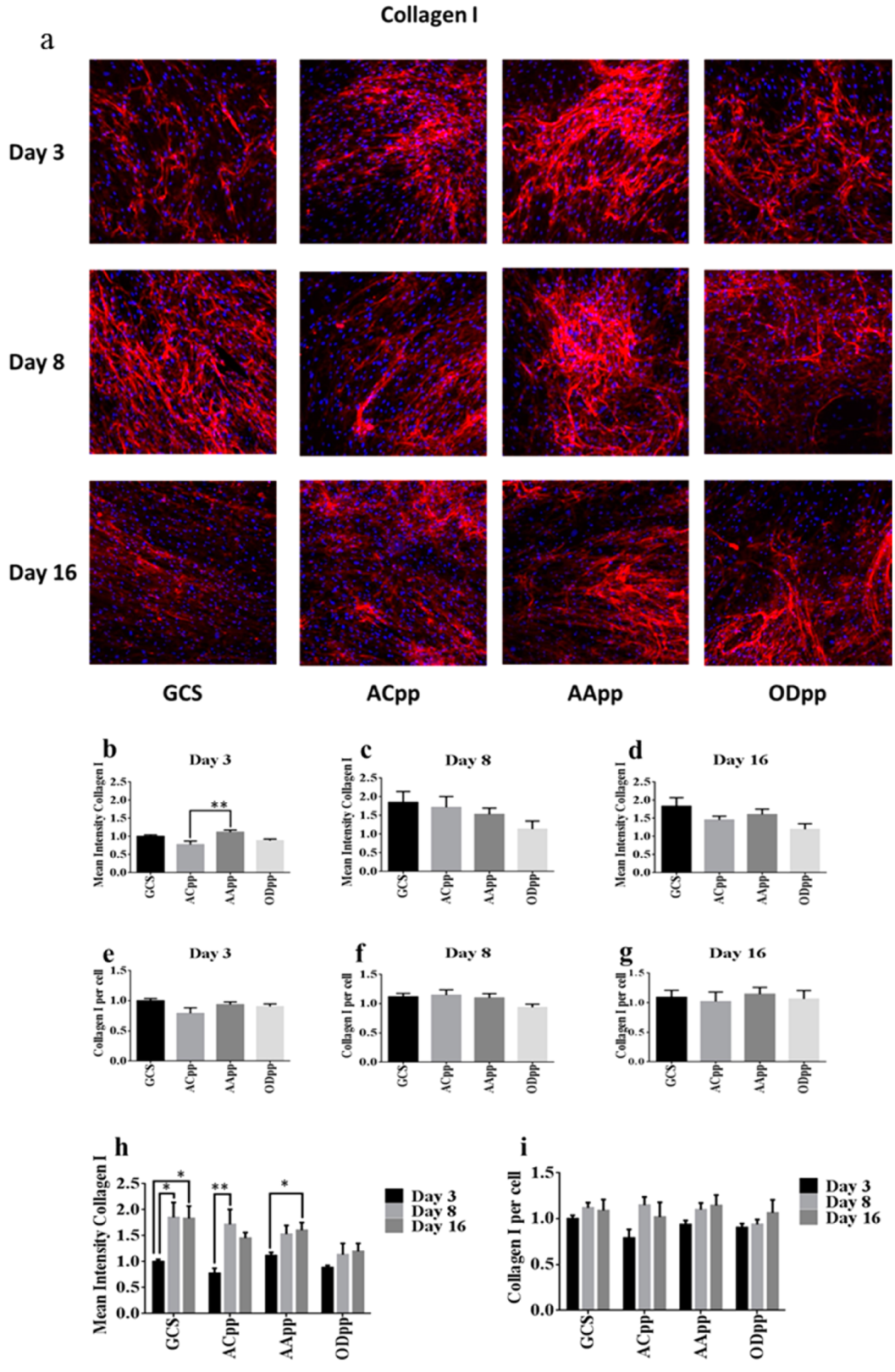

Figure 3. (a) Representative laser scanning confocal microscope images of human dermal fibroblasts and quantification of deposited collagen I on unmodified (GCS) and modified surfaces (ACpp, AApp, and ODpp) at days 3, 8, and 16 (blue: nucleus/DAPI; pink/red: collagen I). All images have dimensions of 1300 × 1300 μm. Quantitative analysis of collagen I deposition obtained from these images. (b–d) Mean intensity of collagen I deposited on unmodified (GCS) and modified surfaces (ACpp, AApp, and ODpp) at days 3, 8, and 16, respectively. (e–g) Amount of collagen I deposited per cell on unmodified (GCS) and modified (ACpp, AApp and ODpp) surfaces at day 3, 8, and 16, respectively. (h) Comparison of mean intensity of collagen I between day 3, 8, and 16. (i) Comparison of collagen I deposition per cell between day 3, 8, and 16. Single asterisk (*) and double asterisks (**) indicate statistical significance $p < 0.05$ and $p < 0.01$, respectively.

DOI: 10.1021/acsami.5b08249
ACS Appl. Mater. Interfaces 2015, 7, 23767–23775

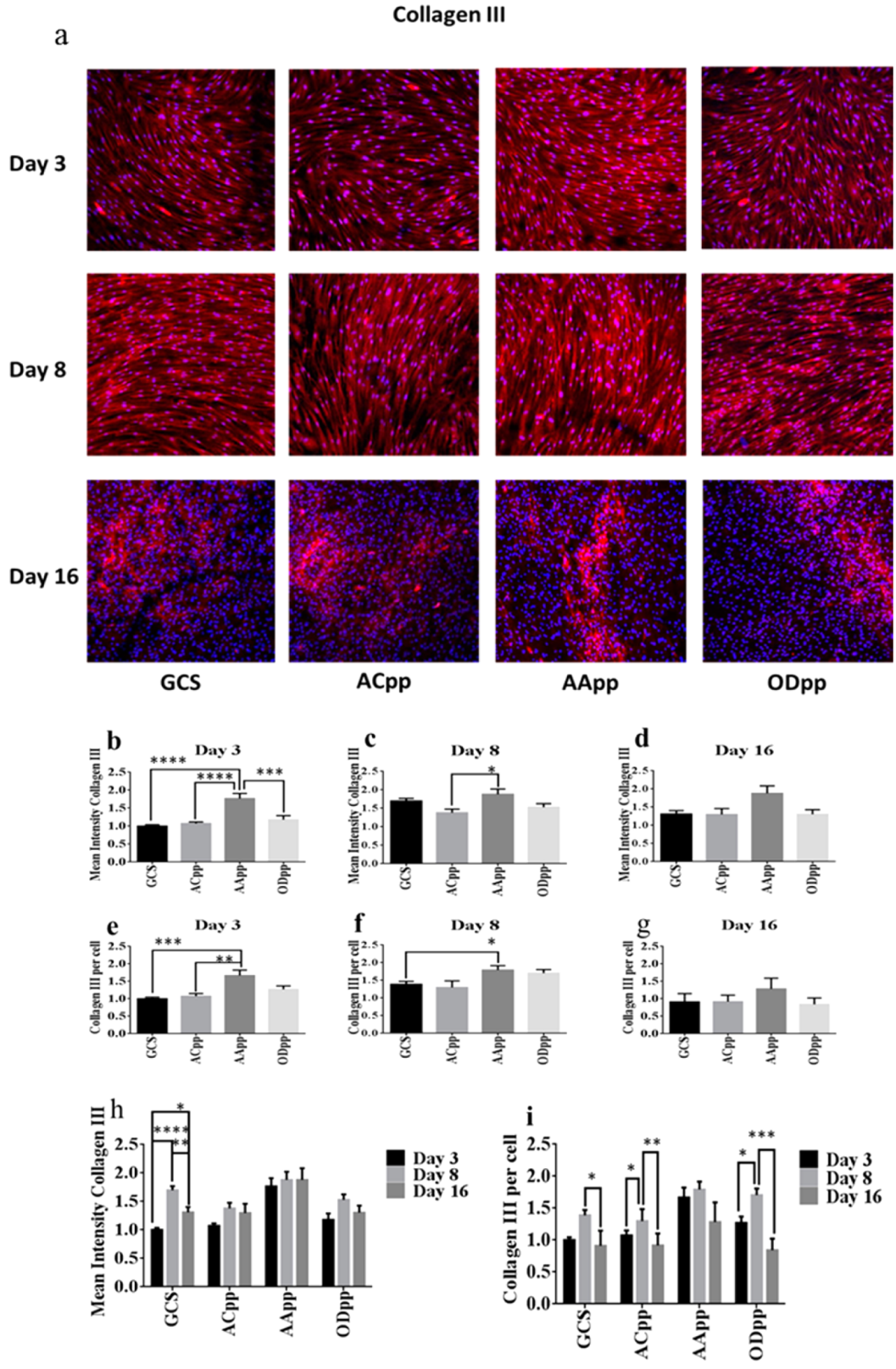

Figure 4. (a) Representative laser scanning confocal microscope images of human dermal fibroblasts and quantification of collagen III on unmodified (GCS) and modified surfaces (ACpp, AApp, and ODpp) at day 3, 8, and 16 (blue, nucleus/DAPI; pink/red, collagen III). All images have dimensions of 1300 × 1300 μm. Quantitative analysis of collagen III obtained from these images. (b–d) show mean intensity of collagen III deposited on unmodified (GCS) and modified surfaces (ACpp, AApp, and ODpp) at days 3, 8, and 16, respectively. (e–g) Amount of collagen III deposited per cell on unmodified (GCS) and modified (ACpp, AApp, and ODpp) surfaces at day 3, 8, and 16 respectively. (h) Comparison of mean intensity of collagen III between day 3, 8, and 16. (i) Comparison of collagen III deposition per cell between day 3, 8, and 16. * = $p < 0.05$, ** = $p < 0.01$, *** = $p < 0.001$ and **** = $p < 0.0001$.

DOI: 10.1021/acsami.5b08249
ACS Appl. Mater. Interfaces 2015, 7, 23767–23775

4i. In the case of ACpp and ODpp surfaces, a significant ($p < 0.05$) increase in collagen III was observed from day 3 to day 8. An increase was also seen in the amount of collagen III produced per cell on the unmodified GCS and the AApp; however, it was not statistically significant. Between days 8 and 16 the amount of collagen III produced per cell decreased on the GCS ($p < 0.05$), ACpp ($p < 0.01$) and ODpp ($p < 0.001$) surfaces. Again the amount of collagen III produced per cell decreased on the AApp surfaces but this was not statistically significant. This decrease in collagen III production at a cellular level appears to be due to the increase in cell number. The number of cells is greatest at day 16, although there are similar amounts of collagen III on days 8 and 16, which accounts for the decrease in the expression of collagen III per cell.

DISCUSSION

In this study, we have demonstrated that surface chemistry can be used to modulate fibroblast growth as well as collagen I and III deposition. Plasma deposition of allylamine (AApp), acrylic acid (ACpp), and octadiene (ODpp) was used to produce coatings with tailored chemical and physical properties. The XPS data confirms the chemical composition for the coatings generated by using these precursors which is consistent with the published data.[33,36,38] Water contact angle measurements showed that surface hydrophobicity increased in the order ACpp < AApp < ODpp. AFM imaging confirmed that the coatings are continuous, pinhole free, and conformal with a RMS below 0.33 nm. This is in agreement with our earlier published reports.[22]

Fibroblasts initially attach better to AApp surfaces than to ODpp surfaces. This can be explained by the higher hydrophobicity of the ODpp, which leads to the adsorption of large amounts of albumin which has been reported to be responsible for reduced cell attachment to surfaces.[39] Faucheux et al. also showed that fibroblasts only weakly attach to CH_3-group-rich surfaces, whereas strong attachment was observed on NH_3- and COOH-rich surfaces.[37] Fibroblasts have also been shown to be sensitive to the density of amine groups on the surface, with increased proliferation observed on surfaces with high concentrations of amine.[36,40]

Although there was no significant difference in cell number on the AApp- and ACpp-coated samples on day 3, production of both collagen I and III was greater on the AApp-coated surfaces compared to the other coatings. However, at later time points (i.e., days 8 and 16), the surface chemistry was shown to have no effect on the production of collagens I and III. Consistent with our findings, in vivo studies by Kamath et al.[41] suggested that amine surfaces show an increase in the thickness of the fibrous capsule and the amount of total cellular infiltrate. Although, how specifically these chemistries can alter the production of collagen I and III was not interrogated.

We also found that collagen III is modulated at a cellular level by surface chemistry. The total collagen III production as well as the amount of collagen III produced per individual cell was strongly elevated on AApp coatings. This clearly shows the importance of surface chemistry for collagen III production. Similarly, collagen I production was higher on AApp than on ODpp-modified surfaces by day 3. A slight decrease was then observed in comparison to the GCS and ACpp surfaces over the course of 16 days. In the case of ODpp surfaces, the collagen I deposition saturated at day 3 and although there was an increase in collagen I deposition, it was not statistically significant over the 16 days of the experiment. These results suggest that surface chemistry can be used to modulate collagen expression after initial implantation. This might aid in the design of improved implantable biomaterial devices.

Surface chemistry is known to affect the adhesion, proliferation, and migration of a variety of cells.[3,42−47] However, the effect of surface chemistry on the deposition of both collagen I and III has not been explored. Surface chemistry is also known to affect protein adsorption to surfaces.[48,49] However, collagen deposition by cells is an active, not a passive process.[50] These data suggest that AApp, a moderately hydrophobic surface, either encourages fibroblasts to produce more collagen I and III or is more energetically favorable for collagen deposition in early stage of growth.

Fibrosis and fibrous capsule formation are inevitable part of the wound healing process, indicative of a chronic stage of inflammation.[41,50−53] Current strategies to minimize this involve disguising the implant material with the use of extremely hydrophilic coatings i.e. poly(ethylene glycol) (PEG) or phosphorylcholine[54,55] or decorating the surface with biomolecules.[56−59] These data suggest that specific surface modification may be a viable and cost-effective path to reduce the formation of a fibrous capsule. The application of an acid chemistry, i.e., an acrylic acid plasma polymer can reduce the amount of both collagen I and III deposition. Alternatively, if increased collagen deposition is needed, i.e., in a dermal replacement material, an amine-rich plasma polymer might be appropriate.

CONCLUSION

We have utilized three types of controlled and tailored chemistries produced by plasma deposition, i.e., amine, carboxyl, and methyl rich. This technique for surface modification was used because of its capacity to deposit thin, conformal coatings on any type of substrate material. We have shown that fibroblasts initially adhere better on amine-rich surfaces. In addition, the initial collagen I and III production is greater on the AApp coatings. Collagen III production initially increased until day 8 and then decreased until day 16, with collagen I production continuously increasing over time. This suggests that collagen III is being replaced by collagen I over time. Collectively, we show the capabilities of surface chemical modification to modulate fibroblast adhesion and collagen I and III production. This study provides useful pioneering knowledge that could help in tuning fibrous capsule formation and in turn govern the fate of implantable biomaterial devices. We anticipate that future exploration in this field will aid in designing biomaterial implants with tailored surface characteristics that will enhance their function to obtain better clinical outcomes.

ASSOCIATED CONTENT

Supporting Information

The Supporting Information is available free of charge on the ACS Publications website at DOI: 10.1021/acsami.5b08249.

Quantitative analysis of laser confocal microscopy images, relative number of fibroblasts on day 3, 8, and 16 (Figure S1a−c); combined relative number of cells on day 3, 8, and 16 (Figure S1d); schematic of parallel plate plasma reactor (Figure S2) (PDF)

DOI: 10.1021/acsami.5b08249
ACS Appl. Mater. Interfaces 2015, 7, 23767−23775

AUTHOR INFORMATION

Corresponding Authors

*E-mail: louise.smith@unisa.edu.au. Phone: (61) 8 8302 1202. Fax: (61) 8 8302 2389.

*E-mail: krasimir.vasilev@unisa.edu.au. Phone: (61) 8 8302 5697. Fax: (61) 8 8302 5689.

Author Contributions

The manuscript was written through contributions of all authors. All authors have given approval to the final version of the manuscript.

Notes

The authors declare no competing financial interest.

ACKNOWLEDGMENTS

The authors thank Professor Michael Roberts at the School of Pharmacy, University of South Australia, for help with the sourcing and collection of the skin. K.V. and J.H. thank to ARC Grant ARC DP15104212.

REFERENCES

(1) Anderson, J. M. Biological Responses to Materials. *Annu. Rev. Mater. Res.* **2001**, *31* (1), 81−110.

(2) Anderson, J. M. Inflammatory Response to Implants. *ASAIO J.* **1988**, *34* (2), 101−107.

(3) Anderson, J. M.; Rodriguez, A.; Chang, D. T. Foreign Body Reaction to Biomaterials. *Semin. Immunol.* **2008**, *20* (2), 86−100.

(4) Ward, W. K. A Review of the Foreign-Body Response to Subcutaneously-Implanted Devices: The Role of Macrophages and Cytokines in Biofouling and Fibrosis. *J. Diabetes Sci. Technol.* **2008**, *2* (5), 768−777.

(5) Castro, P. R.; Marques, S. M.; Campos, P. P.; Cardoso, C. C.; Sampaio, F. P.; Andrade, S. P. Kinetics of Implant-Induced Inflammatory Angiogenesis in Abdominal Muscle Wall in Mice. *Microvasc. Res.* **2012**, *84* (1), 9−15.

(6) Stadelmann, W. K.; Digenis, A. G.; Tobin, G. R.; Physiology. and Healing Dynamics of Chronic Cutaneous Wounds. *Am. J. Surg.* **1998**, *176* (2), 26S−38S.

(7) Hurme, T.; Kalimo, H.; Sandberg, M.; Lehto, M.; Vuorio, E. Localization of Type I and III Collagen and Fibronectin Production in Injured Gastrocnemius Muscle. *Lab. Invest.* **1991**, *64* (1), 76−84.

(8) Lehto, M.; Sims, T.; Bailey, A. Skeletal Muscle Injury—Molecular Changes in the Collagen during Healing. *Res. Exp. Med.* **1985**, *185* (2), 95−106.

(9) Dale, P. D.; Sherratt, J. A.; Maini, P. K. A Mathematical Model for Collagen Fibre Formation during Foetal and Adult Dermal Wound Healing. Proceedings of the Royal Society of London. *Proc. R. Soc. London, Ser. B* **1996**, *263* (1370), 653−660.

(10) Perry, L.; Karp, F.; Hauch, K.; Ratner, B. D. Explanted Pacemakers: Observations of the Long-Term Foreign Body Response. *Interface* **2007**, *4*, 13−21.

(11) Klueh, U.; Kaur, M.; Qiao, Y.; Kreutzer, D. L. Critical Role of Tissue Mast Cells in Controlling Long-Term Glucose Sensor Function In Vivo. *Biomaterials* **2010**, *31* (16), 4540−4551.

(12) Koh, A.; Nichols, S. P.; Schoenfisch, M. H. Glucose Sensor Membranes for Mitigating the Foreign Body Response. *J. Diabetes Sci. Technol.* **2011**, *5* (5), 1052−1059.

(13) Novak, M.; Yuan, F.; Reichert, W. Modeling the Relative Impact of Capsular Tissue Effects on Implanted Glucose Sensor Time Lag and Signal Attenuation. *Anal. Bioanal. Chem.* **2010**, *398* (4), 1695−1705.

(14) Wilson, G. S.; Zhang, Y. *Introduction to the Glucose Sensing Problem*; John Wiley & Sons: Hoboken, NJ, 2009; Vol. *174*, pp 1−27.

(15) Kyle, D. J. T.; Oikonomou, A.; Hill, E.; Bayat, A. Development and Functional Evaluation of Biomimetic Silicone Surfaces with Hierarchical Micro/Nano-Topographical Features Demonstrates Favorable In Vitro Foreign Body Response of Breast-Derived Fibroblasts. *Biomaterials* **2015**, *52* (0), 88−102.

(16) Junge, K.; Klinge, U.; Rosch, R.; Mertens, P. R.; Kirch, J.; Klosterhalfen, B.; Lynen, P.; Schumpelick, V. Decreased Collagen Type I/III Ratio in Patients with Recurring Hernia after Implantation of Alloplastic Prostheses. *Langenbeck's Archives of Surgery* **2004**, *389* (1), 17−22.

(17) Klinge, U.; Si, Z.; Zheng, H.; Schumpelick, V.; Bhardwaj, R.; Klosterhalfen, B. Abnormal Collagen I to III Distribution in the Skin of Patients with Incisional Hernia. *Eur. Surg. Res.* **2000**, *32* (1), 43−48.

(18) Anderson, J.; Defife, K.; McNally, A. Monocyte, Macrophage and Foreign Body Giant Cell Interactions with Molecularly Engineered Surfaces. *J. Mater. Sci.: Mater. Med.* **1999**, *10* (10−11), 579−588.

(19) Christo, S. N.; Diener, K. R.; Bachhuka, A.; Vasilev, K.; Hayball, J. D. Innate Immunity and Biomaterials at the Nexus: Friends or Foes. *BioMed Res. Int.* **2015**, *2015*, 1−23.

(20) Bachhuka, A.; Christo, S. N.; Cavallaro, A.; Diener, K. R.; Mierczynska, A.; Smith, L. E.; Marian, R.; Manavis, J.; Hayball, J. D.; Vasilev, K. Hybrid Core/Shell Microparticles and their use for Understanding Biological Processes. *J. Colloid Interface Sci.* **2015**, *457*, 9−17.

(21) Rinsch, C. L.; Chen, X. L.; Panchalingam, V.; Eberhart, R. C.; Wang, J. H.; Timmons, R. B. Pulsed Radio Frequency Plasma Polymerization of Allyl Alcohol: Controlled Deposition of Surface Hydroxyl Groups. *Langmuir* **1996**, *12* (12), 2995−3002.

(22) Michelmore, A.; Martinek, P.; Sah, V.; Short, R. D.; Vasilev, K. Surface Morphology in the Early Stages of Plasma Polymer Film Growth from Amine-Containing Monomers. *Plasma Processes Polym.* **2011**, *8* (5), 367−372.

(23) Vasilev, K.; Michelmore, A.; Griesser, H. J.; Short, R. D. Substrate Influence on the Iinitial Growth Phase of Plasma-Deposited Polymer Films. *Chem. Commun.* **2009**, *24*, 3600−3602.

(24) Von Keudell, A.; Benedikt, J. A Physicist's Perspective on "Views on Macroscopic Kinetics of Plasma Polymerization. *Plasma Processes Polym.* **2010**, *7*, 376−379.

(25) Gleason, K. K. A Chemical Engineering Perspective on "Views on Macroscopic Kinetics of Plasma Polymerization. *Plasma Processes Polym.* **2010**, *7*, 380−381.

(26) Michelmore, A.; Steele, D. A.; Whittle, J. D.; Bradley, J. W.; Short, R. D. Nanoscale Deposition of Chemically Functionalized Films via Plasma Polymerization. *RSC Adv.* **2013**, *3*, 13540−57.

(27) Vasilev, K.; Michelmore, A.; Martinek, P.; Chan, J.; Sah, V.; Griesser, H. J.; Short, R. D. Early Stages of Growth of Plasma Polymer Coatings Deposited from Nitrogen-and Oxygen-Containing Monomers. *Plasma Processes Polym.* **2010**, *7* (9−10), 824−835.

(28) Stalder, A. F.; Kulik, G.; Sage, D.; Barbieri, L.; Hoffmann, P. A Snake-Based Approach to Accurate Determination of Both Contact Points and Contact angles. *Colloids Surf., A* **2006**, *286* (1−3), 92−103.

(29) MacNeil, S.; Shepherd, J.; Smith, L. Production of Tissue-Engineered Skin and Oral Mucosa for Clinical and Experimental Use. In *3D Cell Culture*; Haycock, J. W., Ed.; Humana Press: New York, 2011; Vol. *695*, pp 129−153.

(30) Chen, C.; Loe, F.; Blocki, A.; Peng, Y.; Raghunath, M. Applying Macromolecular Crowding to Enhance Extracellular Matrix Deposition and its Remodeling In Vitro for Tissue Engineering and Cell-Based Therapies. *Adv. Drug Delivery Rev.* **2011**, *63* (4−5), 277−290.

(31) Chen, C. Z. C.; Peng, Y. X.; Wang, Z. B.; Fish, P. V.; Kaar, J. L.; Koepsel, R. R.; Russell, A. J.; Lareu, R. R.; Raghunath, M. The Scar-in-a-Jar: Studying Potential Antifibrotic Compounds from the Epigenetic to Extracellular Level in a Single Well. *Br. J. Pharmacol.* **2009**, *158* (5), 1196−1209.

(32) Kumar, P.; Satyam, A.; Fan, X.; Collin, E.; Rochev, Y.; Rodriguez, B. J.; Gorelov, A.; Dillon, S.; Joshi, L.; Raghunath, M.; Pandit, A.; Zeugolis, D. I. Macromolecularly Crowded In Vitro Microenvironments Accelerate the Production of Extracellular Matrix-Rich Supramolecular Assemblies. *Sci. Rep.* **2015**, *5*, 8729.

(33) Bullett, N. A.; Whittle, J. D.; Short, R. D.; Douglas, C. I. Adsorption of Immunoglobulin G to Plasma-Co-Polymer Surfaces of Acrylic Acid and 1, 7-Octadiene. *J. Mater. Chem.* **2003**, *13* (7), 1546−1553.

DOI: 10.1021/acsami.5b08249
ACS Appl. Mater. Interfaces 2015, 7, 23767−23775

(34) Mierczynska, A.; Michelmore, A.; Tripathi, A.; Goreham, R. V.; Sedev, R.; Vasilev, K. pH-Tunable Gradients of Wettability and Surface Potential. *Soft Matter* **2012**, *8* (32), 8399−8404.
(35) Goreham, R. V.; Short, R. D.; Vasilev, K. Method for the Generation of Surface-Bound Nanoparticle Density Gradients. *J. Phys. Chem. C* **2011**, *115* (8), 3429−3433.
(36) Hamerli, P.; Weigel, T.; Groth, T.; Paul, D. Surface Properties of and Cell Adhesion onto Allylamine-Plasma-Coated Polyethylenterephtalat Membranes. *Biomaterials* **2003**, *24* (22), 3989−3999.
(37) Faucheux, N.; Schweiss, R.; Lützow, K.; Werner, C.; Groth, T. Self-Assembled Monolayers with Different Terminating Groups as Model Substrates for Cell Adhesion Studies. *Biomaterials* **2004**, *25* (14), 2721−2730.
(38) Parry, K. L.; Shard, A. G.; Short, R. D.; White, R.; Whittle, J. D.; Wright, A. ARXPS Characterization of Plasma Polymerised Surface Chemical Gradients. *Surf. Interface Anal.* **2006**, *38* (11), 1497−1504.
(39) Mager, M. D.; LaPointe, V.; Stevens, M. M. Exploring and Exploiting Chemistry at the Cell Surface. *Nat. Chem.* **2011**, *3* (8), 582−589.
(40) Mitchell, E.; Smith, L. E. Cell Responses to Plasma Polymers - Implications for Wound Care. *Wound Practice Res.* **2012**, *20* (2), 74−79.
(41) Kamath, S.; Bhattacharyya, D.; Padukudru, C.; Timmons, R. B.; Tang, L. Surface Chemistry Influences Implant-Mediated Host Tissue Responses. *J. Biomed. Mater. Res., Part A* **2008**, *86A* (3), 617−626.
(42) Doran, M. R.; Mills, R. J.; Parker, A. J.; Landman, K. A.; Cooper-White, J. J. A Cell Migration Device that Maintains a Defined Surface with no Cellular Damage during Wound Edge Generation. *Lab Chip* **2009**, *9* (16), 2364−2369.
(43) Tang, L.; Hu, W.; Thevenot, P. Surface Chemistry Influences Implant Biocompatibility. *Curr. Top. Med. Chem.* **2008**, *8* (4), 270−280.
(44) Daw, R.; Brook, I. M.; Devlin, A. J.; Short, R. D.; Cooper, E.; Leggett, G. J. A Comparative Study of Cell Attachment to Self-Assembled Monolayers and Plasma Polymers. *J. Mater. Chem.* **1998**, *8* (12), 2583−2584.
(45) Daw, R.; O'Leary, T.; Kelly, J.; Short, R. D.; Cambray-Deakin, M.; Devlin, A. J.; Brook, I. M.; Scutt, A.; Kothari, S. Molecular Engineering of Surfaces by Plasma Copolymerization and Enhanced Cell Attachment and Spreading. *Plasmas Polym.* **1999**, *4* (2), 113−132.
(46) Hopp, I.; Michelmore, A.; Smith, L. E.; Robinson, D. E.; Bachhuka, A.; Mierczynska, A.; Vasilev, K. The Influence of Substrate Stiffness Gradients on Primary Human Dermal Fibroblasts. *Biomaterials* **2013**, *34* (21), 5070−5077.
(47) Kirchhof, K.; Groth, T. Surface Modification of Biomaterials to Control Adhesion of Cells. *Clin. Hemorheol. Microcirc.* **2008**, *39* (1−4), 247−51.
(48) Bullett, N. A.; Whittle, J. D.; Short, R. D.; Douglas, C. W. I. Adsorption of Immunoglobulin G to Plasma-Co-Polymer Surfaces of Acrylic Acid and 1,7-Octadiene. *J. Mater. Chem.* **2003**, *13* (7), 1546−1553.
(49) Siow, K. S.; Britcher, L.; Kumar, S.; Griesser, H. J. Plasma Methods for the Generation of Chemically Reactive Surfaces for Biomolecule Immobilization and Cell Colonization - A Review. *Plasma Processes Polym.* **2006**, *3* (6−7), 392−418.
(50) Chen, C. Z. C.; Raghunath, M. Focus on Collagen: In Vitro Systems to Study Fibrogenesis and Antifibrosis _ state of the art. *Fibrog. Tissue Repair* **2009**, *2* (1), 1−10.
(51) Holt, D. J.; Grainger, D. W. Multinucleated Giant Cells from Fibroblast Cultures. *Biomaterials* **2011**, *32* (16), 3977−3987.
(52) Tang, L.; Eaton, J. W. Inflammatory Responses to Biomaterials. *Am. J. Clin. Pathol.* **1995**, *103* (4), 466−471.
(53) Wick, G.; Grundtman, C.; Mayerl, C.; Wimpissinger, T. F.; Feichtinger, J.; Zelger, B.; Sgonc, R.; Wolfram, D. The Immunology of Fibrosis. *Annu. Rev. Immunol.* **2013**, *31*, 107−135.
(54) Goreish, H. H.; Lewis, A. L.; Rose, S.; Lloyd, A. W. The Effect of Phosphorylcholine-Coated Materials on the Inflammatory Response and Fibrous Capsule Formation: In Vitro and In Vivo Observations. *J. Biomed. Mater. Res.* **2004**, *68A* (1), 1−9.
(55) Wang, L.; Sun, B.; Ziemer, K. S.; Barabino, G. A.; Carrier, R. L. Chemical and Physical Modifications to Poly(Dimethylsiloxane) Surfaces Affect Adhesion of Caco-2 cells. *J. Biomed. Mater. Res., Part A* **2010**, *93* (4), 1260−1271.
(56) Geelhood, S. J.; Horbett, T. A.; Ward, W. K.; Wood, M. D.; Quinn, M. J. Passivating Protein Coatings for Implantable Glucose Sensors: Evaluation of Protein Retention. *J. Biomed. Mater. Res., Part B* **2007**, *81B* (1), 251−260.
(57) Amiji, M.; Park, H.; Park, K. Study on the Prevention of Surface-Induced Platelet Activation by Albumin Coating. *J. Biomater. Sci., Polym. Ed.* **1992**, *3* (5), 375−388.
(58) Morais, J. M.; Papadimitrakopoulos, F.; Burgess, D. J. Biomaterials/Tissue Interactions: Possible Solutions to Overcome Foreign Body Response. *AAPS J.* **2010**, *12* (2), 188−196.
(59) Bridges, A. W.; García, A. J. Biocompatibility of Implanted Diabetes Devices: Part 2: Anti-Inflammatory Polymeric Coatings for Implantable Biomaterials and Devices. *J. Diabetes Sci. Technol.* **2008**, *2* (6), 984−994.

DOI: 10.1021/acsami.5b08249
ACS Appl. Mater. Interfaces 2015, 7, 23767−23775